PHYSICAL REVIEW B **91**, 014422 (2015)

Generalization of polarized spin excitations for asymmetric dimeric systems

G. Houchins and J. T. Haraldsen[*]

Department of Physics and Astronomy, James Madison University, Harrisonburg, Virginia 22807, USA

(Received 22 August 2014; revised manuscript received 4 October 2014; published 16 January 2015)

Through the use of Heisenberg spin-spin interactions, we provide analytical representations for inelastic neutron scattering eigenstates and excitation cross sections of the general S_1-S_2 spin dimeric systems. Using an exact diagonalization approach to the spin Hamiltonian, we analyze various spin coefficients to provide general representations for the neutron scattering cross sections of two interacting spins. We also provide a generalized method for the determination of S_z-polarized excitations, which produces an approximation for the spin excitations within an applied z-axis magnetic field. These calculations enhance the general understanding of the interactions between two individual or compound spin systems, which can help provide insight into condensed matter systems such as molecular magnets, quantum dots, and spintronic systems, as well as particle physics investigations into quark matter and meson interactions.

DOI: 10.1103/PhysRevB.91.014422 PACS number(s): 75.30.Et, 75.50.Ee, 75.50.Xx, 78.70.Nx

I. INTRODUCTION

The study of quantum nanomagnets has been expanding rapidly due to the possible technological applications for systems such as molecular magnets and quantum dots as well as to the presence of quantum tunneling phenomena and anisotropic effects [1–10]. The complete understanding of quantum excitations and the ability to detect and observe them are two critical components for the development of applications in spintronics and spin switches for quantum computation and various device applications [10,11].

Molecular magnets are clusters of magnetic ions that are typically isolated from long-range magnetic interactions by nonmagnetic ligands [12–19], and they typically have many magnetic ions such as Mn_{12} and V_{15} [15,16]. Recently, it has been shown that many excitations within large magnetic clusters are governed by individual subgeometry (smaller two- and three-body components) excitations [20]. Therefore, examining the smallest components of magnetic interactions is critical for moving forward in gaining information for the larger and more complex systems.

From an experimental point of view, there are many techniques that can be employed to characterize and measure the properties of antiferromagnetic spin systems. These include magnetic susceptibility, inelastic neutron scattering (INS), optical/Raman spectroscopy, and electron spin resonance [19,21,22]. While many of these techniques are important for the study of the bulk properties for magnetic systems, INS provides the unique ability to investigate individual excitations and examine local interactions and structural data.

Typically, discussions of magnetic clusters are limited to specific material systems [23–29], which does not always provide a complete picture of the interactions being studied. Spin-$1/2$ clusters have been studied in great detail by a number of theoretical and experimental groups [30–35]. With regards to the spin dimer, Whangbo *et al.* present a detailed analysis of general excitations [31]; however, this work does not examine the changes in the inelastic neutron scattering intensities. Recently, Furrer and Waldman published a systematic review of symmetric S magnetic clusters [36]. However, because mixed valency is common within molecular magnets, it is of great importance to understand not only how symmetric systems work, but also what effects are produced by spin asymmetry and what roles are played in molecular magnets. Therefore, an examination of the spin transitions for excitations of asymmetric magnetic dimer systems is needed.

In this article, we discuss the spin excitations for the general S_1-S_2 dimer system. We evaluate these systems within the context of an isotropic Heisenberg Hamiltonian and determine analytical representations for the eigenstates. We also provide a generalized representation for the unpolarized and polarized INS structure factor for excitations from the ground state and first excited state of any spin dimer configuration. These results allow for a generalized method to determine z-polarized excitations, which can be observed through z-axis magnetic-field and/or single-ion anisotropy splitting, since they will split degenerate states without producing mixing between spin states. Therefore, the unpolarized average will produce subsequent excitations, which for mixed-valence systems will produce multiple excitations with varying intensities. Analysis of these intensity ratios allows for easy characterization of dimeric systems as well as larger molecular magnet systems. We provide detailed examples of these methodologies in the Appendices.

II. SPIN EXCITATIONS FOR MAGNETIC DIMERS

To determine specific individual excitation information, including energy and momentum dependence, one needs to look towards INS. In materials with long-range magnetic ordering, the energy transfer ω is dependent on momentum transfer $\mathbf{q}$, which produces a dispersion relationship. However, for magnetic clusters, there is no dispersion, since excitations are provided in discrete quantum steps. Therefore, to gain specific information about the exchange parameters and magnetic structure, one has to look at the scattering intensity or cross section $S(\mathbf{q},\omega)$ of the excitations.

Typically, magnetic excitations produced by INS follow the selection rule of transition in S_{tot} of ± 1 or 0. However, in cluster and molecular magnet systems, the INS excitations are specific to the spin state being excited. This modification means that neutrons can only excite energy levels of $\Delta S_i = \pm 1$ or 0, where i is the specific basis state of the subgeometries

---

[*] Corresponding author: haraldjt@jmu.edu

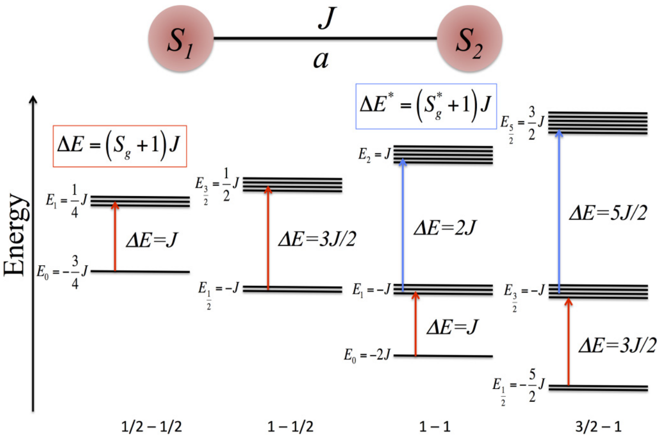

FIG. 1. (Color online) An illustration of the excitations for various spin dimers detailing the ground state and first excited state excitations. Here, we define a spin dimer as the system of any two objects with definite spin separated by distance a and interaction J. Multiple energy level lines denote the number of degenerate states for the level. These will therefore split in magnetic field by $g\mu_B B S_z$.

(typically dimers and trimers). Since each spin state has a specific basis associated with its excitations, the different state excitations are bound by that basis. Within a larger system, individual dimer excitations will always have the same functional form of $1 - \cos(qa)$ multiplied by a structure factor coefficient that is dependent on the specific dimer system that is being excited. Each spin state excited within the dimer determines a unique constant.

To calculate the inelastic neutron scattering excitations for a given magnetic system, a standard Heisenberg Hamiltonian was considered to examine spin-spin exchange correlations for a generalized spin dimer of S_1-S_2. As shown in Fig. 1, the spin dimer consists of two objects with distinct spins that interact through the isotropic Heisenberg interaction, where the Hamiltonian can be written as

$$\mathcal{H} = J\,\mathbf{S}_1 \cdot \mathbf{S}_2 - \mu_B B_z(\mathbf{g}_1 S_{z,1} + \mathbf{g}_2 S_{z,2}), \tag{1}$$

where J is the superexchange parameter between spins $\mathbf{S}_1$ and $\mathbf{S}_2$. The second term shows the application of a z-axis external magnetic field B_z, where $\mathbf{g}$ is the gyromagnetic tensor for each specific magnetic ion, μ_B is the Bohr magneton, and S_z is the z component of the spin operator. From the Hamiltonian, the energy eigenstates and eigenvalues may be found by diagonalizing the magnetic Hamiltonian on a convenient basis. The usual set of $\hat{z}$-polarized magnetic basis states would then be employed. From the Clebsch-Gordon series, the spin decomposition of the general spin dimer is given as

$$\mathbf{S} \otimes \mathbf{S} = \sum_{0}^{S} \mathbf{S}. \tag{2}$$

Therefore, any magnetic state will have $2S_{\text{tot}} + 1$ degenerate states and overall $(2S_1 + 1)(2S_2 + 1)$ total states. The energy eigenstates can be written as a function of the S_{tot} of that state and S_1 and S_2 as given by

$$\begin{aligned} E_{S_{\text{tot}},S_1,S_2} = {} & \tfrac{1}{2}J[S_{\text{tot}}(S_{\text{tot}} + 1) - S_1(S_1 + 1) - S_2(S_2 + 1)] \\ & - E_{Zee} S_z, \end{aligned} \tag{3}$$

where $E_{Zee} = g_{S_z}\mu_B B_z$, and g_{S_z} is a linear combination of the local $\boldsymbol{g}$ tensors [19]. While the $\boldsymbol{g}$ tensors can produce a spin mixing between states, there typically has to be a large crystal-field or aniostropic effect, which is not considered in this model. Therefore, we are considering only states that have little or no spin mixing. As illustrated in Fig. 1, any excitation from a S_{tot} state in the dimer is given by

$$\Delta E = (S_{\text{tot}} + 1)J - E_{Zee}\big(S_z^2 - S_z^1\big), \tag{4}$$

where S_z^i is the magnetic quantum number for each state.

Once the energy eigenstates of the system have been determined, the inelastic neutron scattering cross section can be calculated by evaluating the inelastic structure factor $S(\boldsymbol{q},\omega)$. It should be noted that the applied field will produce a Zeeman shift in the $S_z > 0$ energy levels and produces critical fields that will alter the overall spin ground state. As the Zeeman shift pushes high spin states to lower energy, the system transitions towards a ferromagnetic ground state. The first critical field occurs at

$$E_{Zee} = (S_g + 1)J, \tag{5}$$

where S_g is the original spin ground state equal to S_1-S_2 for $S_1 \geqslant S_2$. At this critical field, the first exciting state will become the ground state. Therefore, for clarity, we examine excitations from the first excited state levels as well, since the excitation matrix elements are reversible. However, with increasing field strength, the system will become completely ferromagnetic when

$$E_{Zee} = S_{\text{tot}}^{\max} J, \tag{6}$$

where $S_{\text{tot}}^{\max} = S_1 + S_2$ is the highest total spin for the dimer system.

In "spin only" magnetic neutron scattering, the differential cross section for the inelastic scattering of an incident neutron from a magnetic system in an initial state Ψ_i, with momentum transfer $\hbar\boldsymbol{q}$ and energy transfer $\hbar\omega$, is given by

$$\frac{d^2\sigma}{d\Omega d\omega} = R(\boldsymbol{q}) \sum_{ba} \left(\delta_{ba} - \frac{q_b q_a}{q^2} \right) S_{ba}^{(fi)}(\boldsymbol{q}\,,\omega), \tag{7}$$

where

$$R(\boldsymbol{q}) = (\gamma r_0)^2 \frac{k'}{k} e^{-2W(\boldsymbol{q})}. \tag{8}$$

In the equation above, $\gamma = 1.91$, r_0 is the classical electron radius, and $e^{-2W(\boldsymbol{q})}$ is the Debye-Waller factor [22,36]. For transitions between discrete energy levels, the standard time integral gives a trivial delta function in the energy transfer. Therefore, for cluster excitations, the energy component can be pulled out and the structure factor becomes dependent only on $\boldsymbol{q}$. Therefore, we define the polarized neutron scattering structure factor

$$\begin{aligned} S_{ba}^{(fi)}(\boldsymbol{q}) = {} & \sum_{\lambda_i,\lambda_f} p_\lambda \langle \Psi_i(\lambda_i)|V_b^\dagger|\Psi_f(\lambda_f)\rangle \\ & \times \langle \Psi_f(\lambda_f)|V_a|\Psi_i(\lambda_i)\rangle, \end{aligned} \tag{9}$$

where the vector $V_a(\boldsymbol{q})$ is a sum of spin operators over all magnetic ions in a unit cell,

$$V_a = \sum_i F_i(\boldsymbol{q}) S_a(\boldsymbol{x}_i)\, e^{i\boldsymbol{q}\cdot\boldsymbol{x}_i}. \tag{10}$$

Here, $F_i(\boldsymbol{q})$ is the normalized spin density for each magnetic moment and p_λ is the thermal population factor which is described by

$$p_\lambda = \frac{1}{Z} e^{-\frac{E_\lambda}{k_B T}}. \tag{11}$$

This provides a temperature dependence on the magnetic excitations. However, it should be mentioned that as temperature increases, the overall structure factor intensity will decrease due to thermal fluctuations until the magnetic order breaks down above a critical thermal energy

$$\begin{aligned} E_{\text{thermal}} &= k_B T_c = \tfrac{1}{2} J \left[S_{\text{tot}}^{\text{max}} \left(S_{\text{tot}}^{\text{max}} + 1 \right) - S_g (S_g + 1) \right] \\ &= J(2S_1 S_2 + S_2). \end{aligned} \tag{12}$$

However, in the case of larger spin dimers, these fluctuations can increase the thermal populations of the first excited state, which can lead to excitations from those higher spin states. However, for simplicity, we assume the system is within the well-established ground state around $T = 0$.

The polarized structure factors describe the excitations for specific z-polarized transitions. However, in the case of a magnetic system with no energy splitting, it is necessary to take an unpolarized average of the polarized bases, which will give the unpolarized structure factor, $\langle S(\boldsymbol{q}) \rangle$. This is an average over the polarized transitions and not a sum due to the probability of populated excitations.

While the aforementioned result applies to neutron scattering from single crystals, many molecular magnetic are actually in powder form. Therefore, to interpret neutron experiments on powder samples, we require an orientation average of the unpolarized single-crystal neutron scattering structure factor. We define this powder average by

$$\bar{S}(q) = \int \frac{d\Omega_{\hat{q}}}{4\pi} S(\boldsymbol{q}). \tag{13}$$

III. UNPOLARIZED STRUCTURE FACTOR COEFFICIENTS

For any dimer excitation, the structure factor always takes on the functional form of

$$S(\boldsymbol{q}) = \bar{\xi}_{S_1,S_2} \left[\frac{F_1^2(\mathbf{q}) + F_2^2(\mathbf{q})}{2} - F_1(\mathbf{q}) F_2(\mathbf{q}) \cos(\boldsymbol{q} \cdot \Delta \boldsymbol{r}) \right], \tag{14}$$

where $F_1(\mathbf{q})$ and $F_2(\mathbf{q})$ are magnetic form factors for each ion and $\bar{\xi}_{S_1,S_2}$ is an unpolarized spin coefficient that is described by averaging the polarized spin correlations $\xi^{|S_1,S_2,S_{\text{tot}}^f,S_z^f\rangle}_{|S_1,S_2,S_{\text{tot}}^i,S_x^i\rangle}$ between all possible initial and final states. If one assumes a symmetric dimer, then the equation is simplified to

$$S(\boldsymbol{q}) = \bar{\xi}_{S_1,S_2} F^2(\mathbf{q}) [1 - \cos(\boldsymbol{q} \cdot \Delta \boldsymbol{r})]. \tag{15}$$

To find the powered averaged structure factor, the integration over all angles simply change $\cos(\boldsymbol{q} \cdot \Delta \boldsymbol{r})$ to $j_0(qa) = \sin(qa)/qa$, where a is the distance between the two interacting spin systems and q is the magnitude of the momentum transfer.

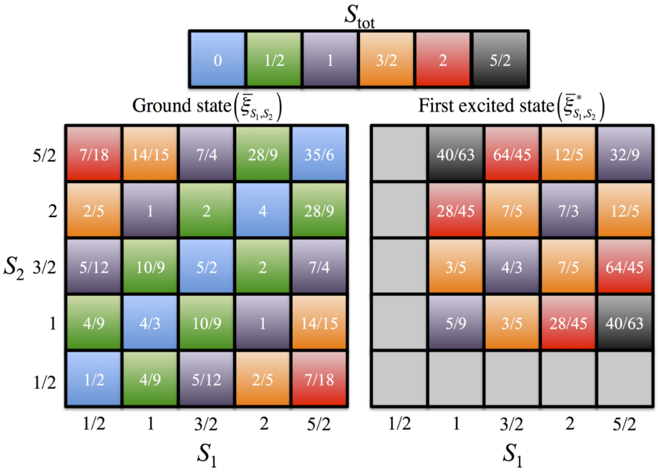

S_{tot}	0	1/2	1	3/2	2	5/2

Ground state $\left(\bar{\xi}_{S_1,S_2}\right)$

S_2 \ S_1	1/2	1	3/2	2	5/2
5/2	7/18	14/15	7/4	28/9	35/6
2	2/5	1	2	4	28/9
3/2	5/12	10/9	5/2	2	7/4
1	4/9	4/3	10/9	1	14/15
1/2	1/2	4/9	5/12	2/5	7/18

First excited state $\left(\bar{\xi}^*_{S_1,S_2}\right)$

S_2 \ S_1	1/2	1	3/2	2	5/2
5/2		40/63	64/45	12/5	32/9
2		28/45	7/5	7/3	12/5
3/2		3/5	4/3	7/5	64/45
1		5/9	3/5	28/45	40/63
1/2					

FIG. 2. (Color online) The INS unpolarized structure factor coefficients grid for the ground state and first excited state excitations in general S_1-S_2 dimer. The colored diagonals denote the various spin ground states from $S_{\text{tot}} = 0$ to 5/2. Larger spin coefficients can be determined by the analytical representations given in Eqs. (16) and (17).

However, by evaluating and examining the polarized matrix coefficients for various dimer combinations and fitting calculated coefficients for specific ground state values to a functional form, an analytical solution for any excitation from the spin ground state $S_g = S_1$-S_2 is deduced by examining correlations between multiple ground state functionals. Therefore, the unpolarized structure factor coefficient can be given by

$$\bar{\xi}_{S_1,S_2} = \frac{2}{3} \frac{S_2(S_1+1)}{S_1 - S_2 + 1}, \tag{16}$$

which provides a generalized formula for any spin combination of S_1 and S_2 using the above expression for S_g and assuming that $S_1 \geqslant S_2$. Furthermore, this methodology allows us to calculate the neutron scattering coefficients for the first excited state, $S_g^* = S_1 - S_2 + 1$. However, the equation varies slightly and can be written as

$$\bar{\xi}^*_{S_1,S_2} = \frac{2}{3} \frac{(S_1 - S_2 + 1)(2S_1 + 3)(2S_2 - 1)}{(S_1 - S_2 + 2)[2(S_1 - S_2) + 3]}. \tag{17}$$

Therefore, dimer excitations from the ground state or the first excited state can be easily determined.

Figure 2 shows the unpolarized neutron scattering coefficient $\bar{\xi}_{S_1,S_2}$ as a function of S_1 and S_2 for excitations from the ground state and the first excited state. Here, the colors of the diagonals indicate the initial total spin state for each transition. These values allow for easy determination of dimeric excitations and provide a better understanding of how the individual spins of the dimer dictate the overall intensity. It is shown that symmetric dimers $S_1 = S_2$ have the largest intensities and deviations from the symmetric configuration will decrease the overall structure factor coefficient. Therefore, if one is examining molecular magnets that consist of multiple dimer configurations (symmetric and asymmetric), then an analysis of the intensity difference can distinguish between them.

Figure 2 also shows the structure factor coefficients for the excitations from the first excited state, $\xi^*_{S_1,S_2}$, where the excited state may have been thermally or electrically populated. Analysis of excited state coefficients can provide increased understanding and characterization of exchange interactions.

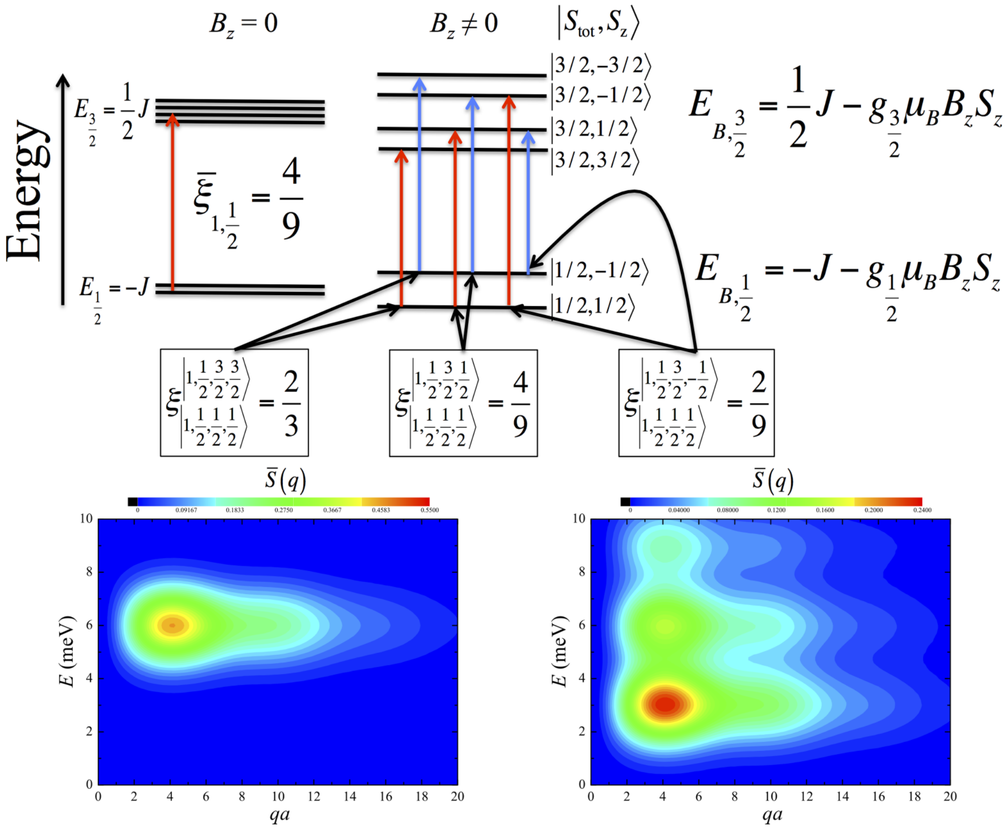

FIG. 3. (Color online) The degenerate energy levels of the 1-1/2 isotropic dimer can be split through the application of an external z axis magnetic field. Here, the spin-1/2 ground state and spin-3/2 excited states shift by the standard Zeeman energy, where $g_{\frac{3}{2}}$ and $g_{\frac{1}{2}}$ denote the mixed valence gyromagnetic tensor constants. The two lower panels show the change in the inelastic neutron scattering spectra for (left) zero field and (right) an applied z-axis magnetic field on a simulated V^{3+}-V^{4+} dimer (spin 1 and spin 1/2), where $J = 4.0$ meV, $\Delta g \mu_B B_z = 1.0$ meV [37]. The magnetic form factor produces a drop off of intensity, but the main peaks remain for comparison.

IV. POLARIZED STRUCTURE FACTOR COEFFICIENTS

While having the unpolarized transition coefficients is useful for understanding the trends and overall describing of isotropic dimer excitations, they provide only information for those single excitations which are typically normalized in inelastic neutron scattering measurement. However, these highly degenerate states are typically split either through the application of a magnetic field (shown in Fig. 3) or a single-ion anisotropy through crystal-field interactions (specifically along the z axis). When these interactions break energy-level degeneracy, then the individual transitions become apparent.

It should be noted that not all applied fields and anisotropies are applicable, because they will produce mixing between spin states, which will affect the eigenfunctions of the spin Hamiltonian. While these affects could be small or negligible, especially in systems with weak anisotropy, it is important to note the distinction.

To determine the coefficient of the structure factor for each possible excitation, we must calculate the probability for each transition from the initial to final spin states, which provides the polarized transitions that are averaged together to get the unpolarized structure factor. These coefficients make up a spin transition matrix (similar to that in Table I.) Here, the matrix contains the information needed for any polarized transition from the $|S^i_{\text{tot}}, S^i_z\rangle$ state to the $\langle S^f_{\text{tot}}, S^f_z|$ state for a specific dimeric system. Because of specific symmetries, only the $\xi^{1,1}$ entry is needed to calculate the unpolarized spin correlation coefficient,

$$\bar{\xi}_{S_1,S_2} = \left\langle S^f_{\text{tot}}, S^f_z \middle| V^+ \middle| S^i_{\text{tot}}, S^i_z \right\rangle^2 \frac{2S^f_{\text{tot}}+1}{3\left(2S^i_{\text{tot}}+1\right)}$$

$$= \xi^{1,1} \frac{2S^f_{\text{tot}}+1}{3\left(2S^i_{\text{tot}}+1\right)}. \quad (18)$$

Therefore, it is useful to be able to determine the polarized matrix coefficients that describe individual transition

TABLE I. Correlation space for excitations between initial and final spin states. The polarized spin correlations coefficients are shown as $\xi^{|S_1,S_2,S^f_{\text{tot}},S^f_z\rangle}_{|S_1,S_2,S^i_{\text{tot}},S^i_z\rangle} = \xi^{m,n}$, where m and n denote the corresponding row and column.

S_1, S_2	$\lvert S^i_{\text{tot}}, S^i_z\rangle$	$\lvert S^i_{\text{tot}}, S^i_z - 1\rangle$	$\cdots$	$\lvert S^i_{\text{tot}}, -S^i_z\rangle$
$\langle S^f_{\text{tot}}, S^f_z\rvert$	$\xi^{1,1}$	$\xi^{1,2}$	$\cdots$	$\xi^{1,2S^i_{\text{tot}}+1}$
$\langle S^f_{\text{tot}}, S^f_z - 1\rvert$	$\xi^{2,1}$	$\xi^{2,2}$	$\cdots$	$\xi^{2,2S^i_{\text{tot}}+1}$
$\vdots$	$\vdots$	$\vdots$		$\vdots$
$\langle S^f_{\text{tot}}, -S^f_z\rvert$	$\xi^{2S^f_{\text{tot}}+1,1}$	$\xi^{2S^f_{\text{tot}}+1,1}$	$\cdots$	$\xi^{2S^f_{\text{tot}}+1,2S^i_{\text{tot}}+1}$

coefficients (illustrated in Fig. 3). Through an analysis of these transitions, the intensity ratios of the split excitations can be used to distinguish and characterize the specific dimer being excited. Typically, these coefficients require a detailed analysis of the eigenstates within the dimer system. However, due to specific symmetries in the coefficient matrix, it is possible to reproduce all transition coefficients through a system of linear equations determined by the unpolarized average and either S_g, for integer ground states, or $\frac{2S_g+1}{2}$, for half-integer ground states, additional starting coefficients. Note that the unpolarized average can be deduced from only the first coefficient in the correlation matrix and the value of the two interacting spins, making these initial conditions very easily attainable. This methodology is discussed in more detail in the appendices, where we provide specific examples for the determination of the coefficients for two spin-dimer combinations. It should be noted that these calculations apply to any spin-dimer system of S_1 and S_2. This includes spin systems with $S > 5/2$. Our analysis in Fig. 2 and the appendices is kept to $S \leqslant 5/2$ because many nanomagnetic materials include only transition-metal elements, for which $S = 5/2$ is applicable. One of our goals is to provide a simplified manner that can be used for larger spin systems, since their calculations can be very tedious. Therefore, our analytical representations for the unpolarized structure factor coefficients [Eqs. (16) and (17)] also hold for systems of $S > 5/2$. The actual numbers are just not given. Furthermore, the methodology for the polarized values also extends to those larger systems.

With the polarized coefficients known, individual excitations can be characterized through z-axis magnetic-field or single-ion anisotropy splitting. Figure 3 shows the degenerate energy levels of the 1-1/2 isotropic dimer being split through the application of an external magnetic field. Here, the single transition is split into six separate transitions as the $S_g = 1/2$ doublet and $S_g^* = 3/2$ quartet are shifted by the applied field (E_{Zee}). Therefore, the unpolarized average coefficient of $\bar{\xi}_{1,1/2} = 4/9$ will split into three polarized coefficients of 2/3, 4/9, and 2/9. This splitting will impact the observed neutron scattering excitations, which is shown in the lower panels of Fig. 3, where an analysis of the INS intensities will allow for the characterization of the spin dimers by looking at the ratios of the individual transition coefficients.

We focus on the isotropic case because it provides the fundamental foundation for all interactions. While many real systems include complex anisotropy and zero-field effects, these interactions tend to be weakly coupled to the overall system. Therefore, any complex spin mixing will be a small perturbation of the isotropic Hamiltonian, and given the resolution limits of many experimental probes (i.e., neutron scattering), the isotropic case is usually a good approximation and beginning metric for the characterization of the systems.

V. CONCLUSION

In conclusion, we provide a detailed understanding of the energy eigenstates and inelastic neutron scattering structure factors for the ground state and first excited state excitations of the generalized S_1-S_2 spin dimer. We provide an analytic representation for the unpolarized structure factors, as well as produce a general methodology for the determination of the individual polarized structure factors, which are needed for systems that have nondegenerate energy levels in the case of anisotropy or the application of a magnetic field. Overall, these calculations can help push the identification and characterization of magnetic systems such as molecular magnets and quantum nanostructures and dots. However, in systems that are beyond the dimer model, larger geometry excitations will affect the energies and structure factor coefficients in various ways. Since large systems are dependent on the subgeometries of the smaller systems, we expect that the ratios of the localized excitation coefficients in those smaller systems should be closely aligned. Therefore, examining the overall effects of other geometries needs further understanding.

While these calculations are performed within the context of condensed matter magnetic systems, the general context and methodology of spin excitations for two interacting spins may be useful for the understanding spin excitations in quark matter, particularly meson excitations [38,39]. The generalization of the spin interactions is independent of probing source and simply investigates the general operations on a local moment.

ACKNOWLEDGMENTS

We would to thank C. Constantin, T. Ahmed, and J.-X. Zhu for useful and insightful discussions.

APPENDIX A: DIMER COEFFICIENT TABLE

To determine the coefficient of the structure factor for each possible excitation, we must calculate the probability for each transition from the initial to final spin states. This provides the polarized transitions, which are then averaged together to get the unpolarized structure factor. These coefficients make up a spin transition matrix (similar to that in Table I). Here, the matrix contains the information needed for any polarized transition from the $|S_{\rm tot}^i, S_z^i\rangle$ state to the $\langle S_{\rm tot}^f, S_z^f|$ state for a specific dimeric system. Because of specific symmetries, only the $\xi^{1,1}$ entry is needed to calculate the unpolarized spin correlation coefficient,

$$\begin{aligned}\bar{\xi}_{S_1,S_2} &= \big\langle S_{\rm tot}^f, S_z^f \big| V^+ \big| S_{\rm tot}^i, S_z^i \big\rangle^2 \frac{2S_{\rm tot}^f + 1}{3\big(2S_{\rm tot}^i + 1\big)} \\ &= \xi^{1,1} \frac{2S_{\rm tot}^f + 1}{3(2S_{\rm tot}^i + 1)}. \end{aligned} \tag{A1}$$

While having the unpolarized transition coefficients is good at describing isotropic dimers, the highly degenerate states can be split either through the application of z-axis magnetic field or single-ion anisotropy. When these energies break energy level degeneracy, the individual transitions become apparent. Therefore, it is useful to be able to easily determine the polarized matrix coefficients. Due to specific symmetries in the coefficient matrix due to the Clebsch-Gordon coefficients, it is possible to reproduce all transition coefficients from only a few coefficient values. Specifically,

$$\xi_{|S_1,S_2,S_{\rm tot}^i,S_z^i\rangle}^{|S_1,S_2,S_{\rm tot}^f,S_z^f\rangle} = \xi_{|S_1,S_2,S_{\rm tot}^i,-S_z^i\rangle}^{|S_1,S_2,S_{\rm tot}^f,-S_z^f\rangle}, \tag{A2}$$

TABLE II. Necessary starting coefficients, by spins, to determine the correlation space matrix.

S_1	S_2	S_g	$\overline{\xi}_{S_1,S_2}$	ξ^{ii}
$\frac{1}{2}$	$\frac{1}{2}$	0	$\frac{1}{2}$	$\frac{1}{2}$
1	$\frac{1}{2}$	$\frac{1}{2}$	$\frac{4}{9}$	$\frac{2}{3}$
$\frac{3}{2}$	$\frac{1}{2}$	1	$\frac{5}{12}$	$\frac{3}{4}$
2	$\frac{1}{2}$	$\frac{3}{2}$	$\frac{2}{5}$	$\frac{4}{5},\frac{12}{25}$
$\frac{5}{2}$	$\frac{1}{2}$	2	$\frac{7}{18}$	$\frac{5}{6},\frac{5}{9}$
1	1	0	$\frac{4}{2}$	$\frac{4}{3}$
$\frac{3}{2}$	1	$\frac{10}{9}$	$\frac{1}{2}$	$\frac{5}{3}$
2	1	1	1	$\frac{9}{5}$
$\frac{5}{2}$	1	$\frac{3}{2}$	$\frac{14}{15}$	$\frac{28}{15},\frac{4}{7}$
$\frac{3}{2}$	$\frac{3}{2}$	0	$\frac{5}{2}$	$\frac{5}{2}$
2	$\frac{3}{2}$	$\frac{1}{2}$	2	$\frac{6}{2}$
$\frac{5}{2}$	$\frac{3}{2}$	1	$\frac{7}{4}$	$\frac{63}{20}$
2	2	0	4	4
$\frac{5}{2}$	2	$\frac{1}{2}$	$\frac{28}{9}$	$\frac{14}{3}$
$\frac{5}{2}$	$\frac{5}{2}$	0	$\frac{35}{6}$	$\frac{35}{6}$

which provides a mirror symmetry to the asymmetric matrix. In addition to this rule, the sum of all row values is given by

$$\sum_{i=1}^{2S^i_{\text{tot}}+1} \xi^{1,i} = \xi^{1,1} \tag{A3}$$

and the sum of all column values gives

$$\sum_{i=1}^{2S^f_{\text{tot}}+1} \xi^{i,1} = 3\overline{\xi}_{S_1,S_2}. \tag{A4}$$

Finally, the diagonal values provide another constraint, which can be written as

$$\sum_{1}^{2S^i_{\text{tot}}+1} \xi^{i,i} = \left(2S^i_{\text{tot}}+1\right)\overline{\xi}_{S_1,S_2}. \tag{A5}$$

With these symmetries, one can produce a system of linear equations for all transition values of $\xi^{m,n}$ given the diagonal values.

APPENDIX B: DIMER COEFFICIENT EXAMPLES

In this section two specific mixed valence dimer situations, $S_1 = 1$, $S_2 = \frac{1}{2}$ and $S_1 = \frac{5}{2}$, $S_2 = \frac{1}{2}$, are discussed in further detail to elaborate the procedure to determine the polarized coefficients. Determination of the average, nonpolarized, coefficient, the use of symmetries of the correlation coefficients, and the implementation of linear equations are all explored through these two examples.

As discussed earlier, the sum of each of the rows of the correlation matrix add to the same number. The top row, however, contains only one value and therefore must be the value the rows add to. Using this information, the value of the first entry, $\xi^{1,1}$, times the number of rows, $2S^f_{\text{tot}}+1$, must equal the sum of all the polarized coefficients. To find the average, note that each column contains 3 and only 3 correlation coefficients. Therefore there are 3 times the number of columns or $3(2S^i_{\text{tot}}+1)$ coefficients. Hence,

$$\begin{aligned}\overline{\xi}_{S_1,S_2} &= \left\langle S^f_{\text{tot}},S^f_z\middle|V^+\middle|S^i_{\text{tot}},S^i_z\right\rangle^2\frac{2S^f_{\text{tot}}+1}{3\left(2S^i_{\text{tot}}+1\right)}\\ &= \xi^{1,1}\frac{2S^f_{\text{tot}}+1}{3\left(2S^i_{\text{tot}}+1\right)}.\end{aligned} \tag{B1}$$

TABLE III. Correlation space for $S_1 = 1$, $S_2 = \frac{1}{2}$ with initial conditions and unknown variables.

	$\langle\frac{1}{2},\frac{1}{2}\vert$	$\langle\frac{1}{2},-\frac{1}{2}\vert$
$\langle\frac{3}{2},\frac{3}{2}\vert$	$\xi^{1,1}=\frac{2}{3}$	0
$\langle\frac{3}{2},\frac{1}{2}\vert$	$\xi^{2,1}$	$\xi^{3,1}$
$\langle\frac{3}{2},-\frac{1}{2}\vert$	$\xi^{3,1}$	$\xi^{2,1}$
$\langle\frac{3}{2},-\frac{3}{2}\vert$	0	$\xi^{1,1}=\frac{2}{3}$

For the case of $S_1 = 1$ and $S_2 = \frac{1}{2}$ only the value of $\xi^{1,1}$ and the average $\overline{\xi}$, which can be deduced from $\xi^{1,1}$, is required to find all polarized constant. From Table II, we find that $\xi^{1,1} = \frac{2}{3}$ and $\overline{\xi} = \frac{4}{9}$.

As shown in Table III, the symmetry

$$\xi^{|S_1,S_2,S^f_{\text{tot}},S^f_z\rangle}_{|S_1,S_2,S^i_{\text{tot}},S^i_z\rangle} = \xi^{|S_1,S_2,S^f_{\text{tot}},-S^f_z\rangle}_{|S_1,S_2,S^i_{\text{tot}},-S^i_z\rangle} \tag{B2}$$

can be used to deduce that

$$\xi^{1,1} = \xi^{4,2} = \tfrac{2}{3}, \quad \xi^{2,1} = \xi^{3,2}, \quad \xi^{3,1} = \xi^{2,2}. \tag{B3}$$

Additionally, the sum of all column values given by

$$\sum_{i=1}^{2S^f_{\text{tot}}+1} \xi^{i,1} = 3\overline{\xi}_{S_1,S_2} \tag{B4}$$

allows us to set up the equation

$$\tfrac{2}{3} + \xi^{2,1} + \xi^{3,1} = \tfrac{4}{3}. \tag{B5}$$

Due to symmetry, there is only one unique equation that can be determined from this condition. The sum of all row values given by

$$\sum_{i=1}^{2S^i_{\text{tot}}+1} \xi^{1,i} = \xi^{1,1} \tag{B6}$$

allows us to set up the equation

$$\xi^{2,1} + \xi^{3,1} = \tfrac{2}{3}, \tag{B7}$$

TABLE IV. Completed correlation space for $S_1 = 1$, $S_2 = \frac{1}{2}$.

	$\langle\frac{1}{2},\frac{1}{2}\vert$	$\langle\frac{1}{2},-\frac{1}{2}\vert$
$\langle\frac{3}{2},\frac{3}{2}\vert$	$\frac{2}{3}$	0
$\langle\frac{3}{2},\frac{1}{2}\vert$	$\frac{4}{9}$	$\frac{2}{9}$
$\langle\frac{3}{2},-\frac{1}{2}\vert$	$\frac{2}{9}$	$\frac{4}{9}$
$\langle\frac{3}{2},-\frac{3}{2}\vert$	0	$\frac{2}{3}$

TABLE V. Correlation space for $S_1 = \frac{5}{2}$, $S_2 = \frac{1}{2}$ with initial conditions and unknown variables.

	$\langle 2,2\rvert$	$\langle 2,1\rvert$	$\langle 2,0\rvert$	$\langle 2,-1\rvert$	$\langle 2,-2\rvert$
$\langle 3,3\rvert$	$\xi^{1,1} = \frac{5}{6}$	0	0	0	0
$\langle 3,2\rvert$	$\xi^{2,1}$	$\xi^{2,2} = \frac{5}{9}$	0	0	0
$\langle 3,1\rvert$	$\xi^{3,1}$	$\xi^{3,2}$	$\xi^{3,3}$	0	0
$\langle 3,0\rvert$	0	$\xi^{4,2}$	$\xi^{4,3}$	$\xi^{4,2}$	0
$\langle 3,-1\rvert$	0	0	$\xi^{3,3}$	$\xi^{3,2}$	$\xi^{3,1}$
$\langle 3,-2\rvert$	0	0	0	$\xi^{2,2} = \frac{5}{9}$	$\xi^{2,1}$
$\langle 3,-3\rvert$	0	0	0	0	$\xi^{1,1} = \frac{5}{6}$

TABLE VI. Completed correlation space for $S_1 = \frac{5}{2}$, $S_2 = \frac{1}{2}$.

	$\langle 2,2\rvert$	$\langle 2,1\rvert$	$\langle 2,0\rvert$	$\langle 2,-1\rvert$	$\langle 2,-2\rvert$
$\langle 3,3\rvert$	$\frac{5}{6}$	0	0	0	0
$\langle 3,2\rvert$	$\frac{5}{18}$	$\frac{5}{9}$	0	0	0
$\langle 3,1\rvert$	$\frac{1}{18}$	$\frac{4}{9}$	$\frac{1}{3}$	0	0
$\langle 3,0\rvert$	0	$\frac{1}{6}$	$\frac{1}{2}$	$\frac{1}{6}$	0
$\langle 3,-1\rvert$	0	0	$\frac{1}{3}$	$\frac{4}{9}$	$\frac{1}{18}$
$\langle 3,-2\rvert$	0	0	0	$\frac{5}{9}$	$\frac{5}{18}$
$\langle 3,-3\rvert$	0	0	0	0	$\frac{5}{6}$

where we have substituted $\xi^{2,2}$ for $\xi^{3,1}$. Again because of symmetry there is only one equation that can be determined from this constraint. The final condition on the values of the diagonals provides no further information since there are 2 unique equations and only 2 unique unknowns. Solving the above system of two equations yields

$$\xi^{2,1} = \xi^{3,2} = \frac{4}{9}, \quad \xi^{2,2} = \xi^{3,1} = \frac{2}{9}.$$

The completed correlation space for $S_1 = 1$, $S_2 = \frac{1}{2}$ is given in Table IV for reference. A more complicated system of equations occurs for $S_1 = \frac{5}{2}$, $S_2 = \frac{1}{2}$. The space matrix is demonstrated in Table V.

From Table II, $\xi^{1,1} = \frac{5}{6}$, $\xi^{2,2} = \frac{5}{9}$, and $\bar{\xi} = \frac{7}{18}$. Similarly to the earlier case, symmetry is used to find that

$$\begin{gathered} \xi^{1,1} = \xi^{7,5} = \frac{5}{6}, \quad \xi^{2,1} = \xi^{6,5}, \\ \xi^{3,1} = \xi^{5,5}, \quad \xi^{2,2} = \xi^{6,4} = \frac{5}{9}, \\ \xi^{3,2} = \xi^{5,4}, \quad \xi^{4,2} = \xi^{4,4}, \\ \xi^{3,3} = \xi^{5,3}. \end{gathered} \tag{B8}$$

Now there are only 5 unique unknowns. The first set of equations is given from the sum of the columns:

$$\frac{5}{6} + \xi^{2,1} + \xi^{3,1} = \frac{7}{6}, \tag{B9}$$

$$\frac{5}{9} + \xi^{3,2} + \xi^{4,2} = \frac{7}{6}, \tag{B10}$$

$$2\xi^{3,3} + \xi^{4,3} = \frac{7}{6}. \tag{B11}$$

The next set of equations comes from the sum of the rows:

$$\xi^{2,1} + \frac{5}{9} = \frac{5}{6}, \tag{B12}$$

$$\xi^{3,1} + \xi^{3,2} + \xi^{3,3} = \frac{5}{6}, \tag{B13}$$

$$2\xi^{4,2} + \xi^{4,3} = \frac{5}{6}. \tag{B14}$$

The final set of equations comes from the diagonal values, which can be written as

$$\sum_{1}^{2S^i_{\text{tot}}+1} \xi^{i,i} = (2S^i_{\text{tot}} + 1)\bar{\xi}_{S_1,S_2}. \tag{B15}$$

This yields the equations

$$\frac{25}{9} + \xi^{3,3} = \frac{14}{9}, \tag{B16}$$

$$2\xi^{2,1} + 2\xi^{3,2} + \xi^{4,3} = \frac{14}{9}. \tag{B17}$$

Therefore, the complete correlation space for $S_1 = \frac{5}{2}$, $S_2 = \frac{1}{2}$ is given in Table VI for reference.

---

[1] E. Dagotto and T. M. Rice, Surprises on the Way from One- to Two-Dimensional Quantum Magnets: The Ladder Materials, Science **271**, 618 (1996).

[2] A. L. Barra, A. Caneschi, A. Cornia, F. Frabrizi de Biani, D. Gatteschi, C. Sangregorio, R. Sessoli, and L. Sorace, Single-Molecule Magnet Behavior of a Tetranuclear Iron(III) Complex. The Origin of Slow Magnetic Relaxation in Iron(III) Clusters, J. Am. Chem. Soc. **121**, 5302 (1999).

[3] D. P. DiVincenzo and D. Loss, Quantum computers and quantum coherence, J. Magn. Magn. Mater. **200**, 202 (1999).

[4] Y. Furukawa, M. Luban, F. Borsa, D. C. Johnston, A. V. Mahajan, L. L. Miller, D. Mentrup, J. Schnack, and A. Bino, Magnetism and spin dynamics in the cluster compound $[Cr_4S(O_2CCH_3)_8(H_2O)_4](NO_3)_2{\cdot}H_2O$, Phys. Rev. B **61**, 8635 (2000).

[5] A. Bouwen, A. Caneschi, D. Gatteschi, E. Goovaerts, D. Schoemaker, L. Sorace, and M. Stefan, Single-Crystal High-Frequency Electron Paramagnetic Resonance Investigation of a Tetranuclear Iron(III) Single-Molecule Magnet, J. Phys. Chem. B **105**, 2658 (2001).

[6] A. Cornia, R. Sessoli, L. Sorace, D. Gatteschi, A. L. Barra, and C. Daiguebonne, Origin of Second-Order Transverse Magnetic Anisotropy in Mn_{12}-Acetate, Phys. Rev. Lett. **89**, 257201 (2002).

[7] D. Mentrup, J. Schnack, and M. Luban, Spin dynamics of quantum and classical Heisenberg dimers, Physica A **272**, 153 (1999).

[8] D. Mentrup, H.-J. Schmidt, J. Schnack, and M. Luban, Transition from quantum to classical Heisenberg trimers: thermodynamics and time correlation functions, Physica A **278**, 214 (2000).

[9] O. Cifta, The irregular tetrahedron of classical and quantum spins subjected to a magnetic field, J. Phys. A **34**, 1611 (2001).

[10] M. A. Nielsen and I. L. Chuang, *Quantum Computation and Quantum Information* (Cambridge University Press, Cambridge, 2000).

[11] P. Tyagi, Molecular Spin Devices: Current Understanding and New Territories, NANO: Brief Reports and Reviews **04**, 325 (2009).

[12] R. M. White, *Quantum Theory of Magnetism: Magnetic Properties of Materials* (Springer, New York, 2010).

[13] D. Gatteschi, R. Sessoli, and J. Villain, *Molecular Nanomagnets* (Oxford University Press, Oxford, 2006).

[14] A. J. Tasiopoulos, A. Vinslava, W. Wernsdorfer, K. A. Abboud, and G. Christou, Giant Single-Molecule Magnets: A $\{Mn_{84}\}$ Torus and Its Supramolecular Nanotubes, Angew. Chem., Int. Ed. **43**, 2117 (2004).

[15] E. del Barco, A. D. Kent, S. Hill, J. M. North, N. S. Dalal, E. M. Rumberger, D. N. Hendrickson, N. Chakov, and G. Christou, Magnetic Quantum Tunneling in the Single-Molecule Magnet Mn_{12}-Acetate, J. Low Temp. Phys. **140**, 119 (2005).

[16] G. Chaboussant, R. Basler, A. Sieber, S. T. Ochsenbein, A. Desmedt, R. E. Lechner, M. T. F. Telling, P. Kgerler, A. Muller, and H.-U. Güdel, Low-energy spin excitations in the molecular magnetic cluster V_{15}, Europhys. Lett. **59**, 291 (2002).

[17] K. R. Dunbar and R. A. Heintz, in *Chemistry of Transition Metal Cyanide Compounds: Modern Perspectives*, Progress in Inorganic Chemistry, Vol. 45, edited by K. D. Karlin (John Wiley & Sons, New York, 2007), p. 283.

[18] M. Shatruk, C. Avendano, and K. R. Dunbar, in *Cyanide-Bridged Complexes of Transition Metals: A Molecular Magnetism Perspective*, Progress in Inorganic Chemistry, Vol. 56, edited by K. D. Karlin (John Wiley & Sons, New York, 2009).

[19] O. Kahn, *Molecular Magnetism* (VCH Publishers, New York, 1993).

[20] J. T. Haraldsen, Heisenberg Pentamer: Insights into Inelastic Neutron Scattering on Magnetic Clusters, Phys. Rev. Lett. **107**, 037205 (2011).

[21] G. L. Squires, *Introduction to the Theory of Thermal Neutron Scattering* (Dover Publications, 1996).

[22] S. W. Lovesey, *Theory of Neutron Scattering from Condensed Matter* (Oxford Science Publishers, Oxford, 1987).

[23] M. Ameduri and R. A. Klemm, Time correlation functions of three classical Heisenberg spins on an isosceles triangle and on a chain, Phys. Rev. B **66**, 224404 (2002).

[24] D. V. Efremov and R. A. Klemm, Heisenberg dimer single molecule magnets in a strong magnetic field, Phys. Rev. B **66**, 174427 (2002).

[25] R. A. Klemm and M. Ameduri, Exact time autocorrelation function of the N-spin classical Heisenberg equivalent neighbor model, Phys. Rev. B **66**, 012403 (2002).

[26] O. Waldmann, Q dependence of the inelastic neutron scattering cross section for molecular spin clusters with high molecular symmetry, Phys. Rev. B **68**, 174406 (2003).

[27] D. A. Tennant, S. E. Nagler, A. W. Garrett, T. Barnes, and C. C. Torardi, Excitation Spectrum and Superexchange Pathways in the Spin Dimer $VODPO_4 \cdot \frac{1}{2}D_2O$, Phys. Rev. Lett. **78**, 4998 (1997).

[28] J. T. Haraldsen, T. Barnes, J. W. Sinclair, J. R. Thompson, R. L. Sacci, and J. F. C. Turner, Magnetic properties of a Heisenberg coupled-trimer molecular magnet: General results and application to spin-1/2 vanadium clusters, Phys. Rev. B **80**, 064406 (2009).

[29] J. T. Haraldsen, M. B. Stone, M. D. Lumsden, T. Barnes, R. Jin, J. W. Taylor, and F. Fernandez-Alonso, Spin-lozenge thermodynamics and magnetic excitations in Na_3RuO_4, J. Phys. Condens.: Matter **21**, 506003 (2009).

[30] J. T. Haraldsen, T. Barnes, and J. L. Musfeldt, Neutron scattering and magnetic observables for $S = 1/2$ spin clusters and molecular magnets, Phys. Rev. B **71**, 064403 (2005).

[31] M. H. Whangbo, H. J. Koo, and D. Dai, Spin exchange interactions and magnetic structures of extended magnetic solids with localized spins: theoretical descriptions on formal, quantitative and qualitative levels, J. Solid State Chem. **176**, 417 (2003).

[32] M. Luban, F. Borsa, S. Budko, P. Canfield, S. Jun, J. K. Jung, P. Kogerler, D. Mentrup, A. Muller, R. Modler, D. Procissi, B. J. Suh, and M. Torikachvili, Heisenberg spin triangles in $\{V_6\}$-type magnetic molecules: Experiment and theory, Phys. Rev. B **66**, 054407 (2002).

[33] B. Cage, F. A. Cotton, N. S. Dalal, E. A. Hillard, B. Ravkin, and C. M. Ramsey, Observation of Symmetry Lowering and Electron Localization in the Doublet-States of a Spin-Frustrated Equilateral Triangular Lattice: $Cu_3(O_2C_{16}H_{23})_6{\cdot}1.2\ C_6H_{12}$, J. Am. Chem. Soc. **125**, 5270 (2003).

[34] B. Cage, F. A. Cotton, N. S. Dalal, E. A. Hillard, B. Ravkin, and C. M. Ramsey, EPR probing of bonding and spin localization of the doublet-quartet states in a spin-frustrated equilateral triangular lattice: $Cu_3(O_2C_{16}H_{23})_6{\cdot}1.2\ C_6H_{12}$, C. R. Chimie **6**, 39 (2003).

[35] U. Kortz, S. Nellutla, A. C. Stowe, N. S. Dalal, J. van Tol, and B. S. Bassil, Structure and Magnetism of the Tetra-Copper(II)-Substituted Heteropolyanion $[Cu_4K_2(H_2O)_8(\alpha\text{-}AsW_9O_{33})_2]^{8-}$, Inorg. Chem. **43**, 144 (2004).

[36] A. Furrer and O. Waldmann, Magnetic cluster excitations, Rev. Mod. Phys. **85**, 367 (2013).

[37] A. J. Dianoux and G. Lander, *Neutron Data Booklet* (OCP Science, Philadelphia, 2003).

[38] F. Osterfeld, Nuclear spin and isospin excitations, Rev. Mod. Phys. **64**, 491 (1992).

[39] S. Krewald and J. Speth, Microscopic Structure of the Magnetic High-Spin States in ^{208}Pb, Phys. Rev. Lett. **45**, 417 (1980).